J. Physiol. (1977), **273**, *pp.* 573–596
With 13 *text-figures*
Printed in Great Britain

INACTIVATION OF SODIUM CHANNELS: SECOND ORDER KINETICS IN MYELINATED NERVE

BY S. Y. CHIU

From the Department of Physiology and Biophysics, SJ-40, University of Washington School of Medicine, Seattle, Washington 98195, U.S.A.

(*Received 29 November 1976*)

SUMMARY

1. Kinetics of inactivation of sodium channels in myelinated nerve from *Rana pipiens* were studied at 4·5 °C using the voltage clamp technique of Dodge & Frankenhaeuser (1958).

2. Potassium currents were blocked by cutting the internodes in 20 mM-TEA-Cl + 100 mM-KCl and by adding 12 mM-TEA-Cl to the external Ringer. Leakage and capacitative currents were subtracted electronically.

3. Kinetics of recovery from inactivation of the sodium channels were studied by inactivating the channels with a large depolarizing prepulse and allowing the channels to recover at different potentials; the extent of recovery was measured by applying a test pulse at various times after the prepulse.

4. Kinetics of development of inactivation were studied by two different methods. The first was to measure the decay of sodium current under a maintained depolarization. The second method was to measure the decay of the peak sodium current in a test pulse as a function of time after the onset of a maintained depolarization. These two methods yielded similar results for the kinetics of inactivation development.

5. Contrary to expectations of the Hodgkin–Huxley formalism, the time course of recovery from and development of inactivation is not strictly exponential. Rather, recovery from complete inactivation shows an initial delay which depends on recovery potentials. Development of inactivation at a fixed potential exhibits at least two exponentials.

6. The steady-state inactivation curve $h_\infty(E)$ is asymmetrical and is fitted better by $1/[1+\exp(A_1E+B_1)+\exp(A_2E+B_2)]$ than by

$$1/[1+\exp(AE+B)].$$

7. Most of the above kinetic observation on inactivation can be fitted

by the following modification of the h system of the Hodgkin–Huxley formalism:

open closed closed

$$0 \underset{a_{10}}{\overset{a_{01}}{\rightleftharpoons}} 1 \underset{a_{21}}{\overset{a_{12}}{\rightleftharpoons}} 2 \quad (a_{ij} = \exp(A_{ij}E + B_{ij}))$$

8. In the analysis it was not necessary to modify the concept of two separate processes, activation and inactivation, governing the opening and closing of the sodium channels.

INTRODUCTION

Twenty years after Hodgkin & Huxley pioneered the concept of a voltage-sensitive gating system in nerve membrane, its precise molecular nature is still unresolved. Recently Hodgkin–Huxley equations (1952*b*) describing the sodium permeability changes have been subjected to re-examination due to discoveries of apparent disagreements on sodium gating kinetics. Two general types of kinetic aberrations have been reported, both relating to the h inactivation system. The first type deals with lags and history-dependent inactivation (Schauf, 1974; Armstrong, 1970; Goldman & Schauf, 1972; Chandler & Meves, 1970; Peganov, 1973). The second type concerns the observation that the rate constants and steady inactivation vary with the methods used to measure them (Goldman & Schauf, 1972, 1973; Hoyt & Adelman, 1970). These observations have been interpreted by some authors (Goldman, 1975; Hoyt & Adelman, 1970) as rendering untenable the concept of two separate processes, m and h, governing the turn-on and -off of the sodium current. Instead, these authors propose a set of coupled equations, schematically very different from the Hodgkin–Huxley equations and with a different physical interpretation concerning the nature of the gating system. Relatively unpursued, however, is the possibility that some of these kinetic aberrations can be accounted for by the hypothesis that inactivation is itself a second order process rather than a first order process (Chandler & Meves, 1970; Hille, 1976).

It seems worthwhile to re-examine the validity of the Hodgkin–Huxley formalism. I have confirmed some but not all of the kinetic deviations reported by some authors and extended some of these observations. The observed kinetics of inactivation were analysed quantitatively in terms of a second order system. It appears that the Hodgkin–Huxley formalism need only be modified in this aspect to account for the kinetic deviations. An abstract of this work has been presented to the Biophysical Society (Chiu, 1976).

METHODS

Nodes of Ranvier of single myelinated fibres from the sciatic nerve of *Rana pipiens* were voltage clamped by the techniques of Dodge & Frankenhaeuser (1958) with modifications by Hille (1971). The dissection and the mounting of the nerve in the plastic chamber took about 1 hr. The chamber with the nerve mounted was put into a brass block maintained at 4·5 °C and the pool bathing the node was immediately perfused with fresh Ringer solution. The node was then stimulated and, if it was excitable, all the amplifiers were turned off and the nerve chamber and electrodes were allowed to stabilize for half an hour before recording started. After the stabilization period, the voltage clamp was applied and the holding membrane potential was adjusted to give a resting inactivation of 0·5–0·7. The holding potentials adjusted in this manner were between −80 and −90 mV. Nodes requiring holding potentials more negative than −90 mV were discarded.

The solution bathing the node was composed of 115 mM-NaCl, 2 mM-$CaCl_2$, 2·5 mM-KCl, 4 mM-Tris-(hydroxymethyl)aminomethane buffer (pH 7·4) with 12 mM tetraethylammonium chloride (TEA-Cl) added to block currents in potassium channels (Hille, 1970). In experiments exploring possible effects of series resistance, low-sodium solutions were made by replacing sodium with an osmotically equivalent amount of tetramethylammonium chloride (TMA-Cl). All solutions were stored in the refrigerator until use.

The ends of the nerve fibre were cut in 100 mM-KCl, plus 20 mM-TEA-Cl. The TEA-Cl diffused via the cut ends of the nerve to the inside of the node and blocked outward potassium currents after some minutes (Koppenhofer & Vogel, 1969; Armstrong & Hille, 1972). Thus, with external and internal TEA-Cl of 12 and 20 mM respectively, the only ionic currents left in voltage clamp were the sodium and leak currents. The leak and capacitative currents were then subtracted off by analogue circuitry to allow direct observation of the sodium currents on the oscilloscope. The oscilloscope traces were recorded on film and analysed later.

General procedures

Three main categories of measurement were made: the time course of development of inactivation, the time course of recovery from inactivation and the steady-state inactivation as a function of membrane voltage. Recovery from inactivation was studied by inactivating Na channels with a 50 msec depolarizing prepulse to −20 mV. Complete inactivation of the sodium current in the prepulse was checked by observing on the oscilloscope that the sodium current decayed to the base line by the end of the prepulse. Within 200 μsec after termination of the prepulse, the membrane was repolarized to different potentials to induce recovery from previous inactivation. The time course of recovery at each recovery potential was measured by applying a test pulse of −10 mV at various time intervals after the prepulse. Immediately after each test pulse, a control pulse was applied which was defined to be a test pulse applied 200 msec after the depolarizing prepulse. The peak sodium current in the control pulse was then used to normalize the preceding test current. The control sodium current for a given recovery potential was checked to make sure that it did not change whether the prepulse was turned on or off. For recovery at very hyperpolarizing voltages, the control pulse was taken at only 20 msec after the prepulse since prolonged hyperpolarization at a very negative value killed the node. In a healthy fibre, a set of recovery measurements at six to eight different potentials could be done within 20 min.

The time course of development of inactivation was measured in two ways. The first method was to impose a step depolarization and measure the decay of the sodium

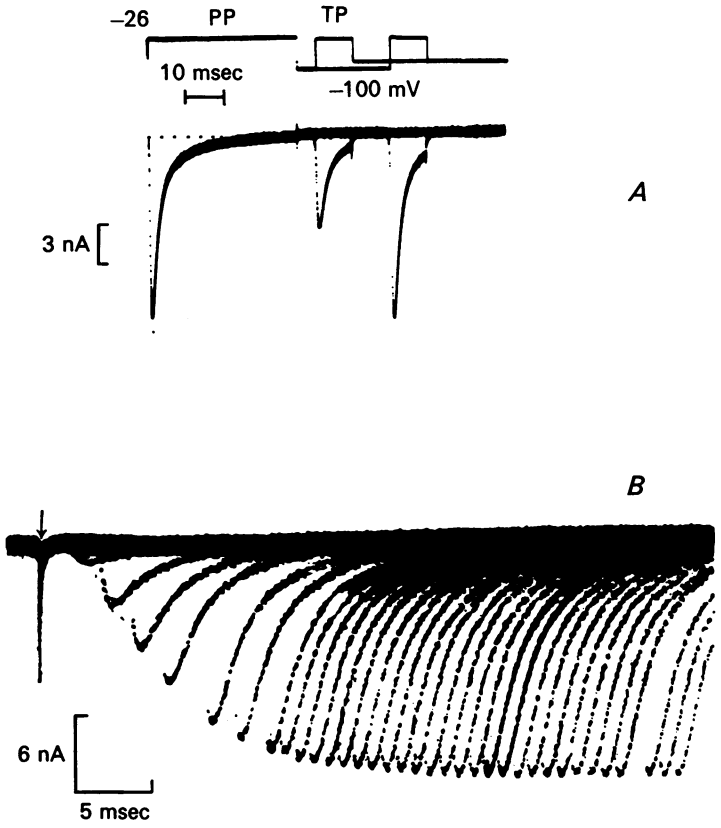

Fig. 1. Direct observation of delay in recovery from inactivation in sodium channels on the oscilloscope screen. Potassium currents were blocked by internal and external application of TEA (see Methods) and leak was subtracted electronically. Part *A* illustrates the two-pulse method. Upper trace, voltage. Lower trace, current. Sodium channels were completely inactivated by a 40 msec prepulse (PP) to −26 mV. Subsequently, the membrane potential was hyperpolarized to −100 mV to permit recovery from inactivation. The degree of recovery at 5 and 25 msec after the prepulse was assayed by applying test pulses (TP) at these times. The size of the peak current in these two test pulses reflects the degree of recovery from previous inactivation. In actual measurement, the peak sodium current in each test pulse was normalized with respect to a test current corresponding to a test pulse taken 200 msec after the prepulse. In *B*, only the last 3 msec of the sodium current in the prepulse is shown. At time marked by the arrow, the prepulse was terminated and the membrane was repolarized to rest (−85 mV). Recovery from inactivation at the resting potential was measured by applying a sequence of test pulses at various times after the prepulse. All the resulting test currents were superimposed and their peaks traced out the time course of recovery. It can be seen that the recovery is sigmoidal with an initial delay of about 3 msec. This run was completed in 10 sec. Node 101. Temperature 4·5 °C.

current under the maintained depolarization. The second method was to apply a test pulse at different intervals after the onset of a step depolarization and to measure the dependence of the peak sodium current on the time after the onset. The time constants of inactivation development for each potential were determined by semi-logarithmic plots of the normalized current time course or peak current amplitudes.

The steady-state inactivation as a function of potential was measured by applying a test pulse after various prepulse potentials lasting 50 msec. This procedure is identical to that first used by Hodgkin & Huxley (1952*a*).

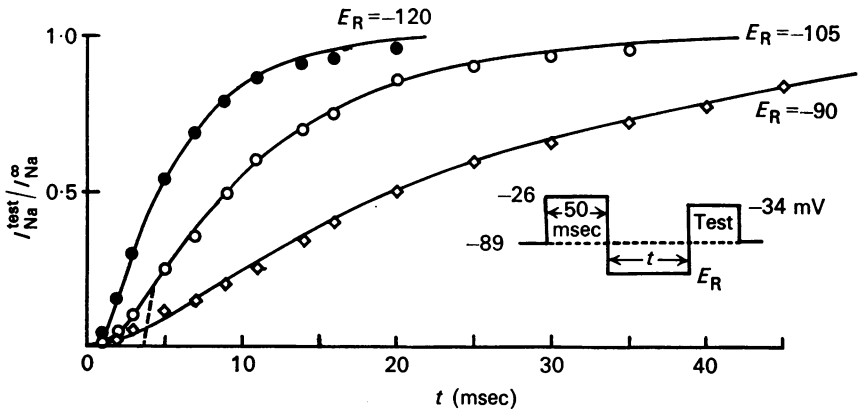

Fig. 2. Quantitative analysis of recovery from complete inactivation at three different potentials. Sodium channels were inactivated by a 50 msec prepulse to −26 mV. Recovery from inactivation at a given potential E_R was measured by applying a test pulse at various times after the prepulse. Abscissa: time interval between end of the prepulse and onset of the test pulse. Ordinate: $I^{test}_{Na}/I^{\infty}_{Na}$, where I^{test}_{Na} is the peak sodium current in the test pulse and I^{∞}_{Na} is the peak sodium current in a test pulse taken 200 msec after the prepulse. ●, ○, ◇: E_R = −120, −105, −90 mV, respectively. Node 38. Resting potential −89 mV. Temperature 4·5 °C. Continuous lines in this Figure (and Fig. 3) are calculated from eqn. (14) using the four rate constants given by eqns. (10)–(13). Figs. 2–5, 10 and 11 show analysed data from the same node, N38.

RESULTS AND ANALYSIS

The observations are best described in terms of the three categories of measurement mentioned in the Methods.

Recovery from inactivation

Recovery was studied with test pulses applied some time after a prepulse as is shown in Fig. 1*A*. In all the recovery experiments, the prepulse was chosen to induce complete inactivation of the sodium current by the end of the prepulse. Contrary to the expectations of the Hodgkin–Huxley scheme, the peak current does not recover exponentially with time at a given recovery potential. Rather, the recovery always shows a

sigmoidal time course with a small initial delay (Fig. 1*B*) as observed by Schauf (1974) on *Myxicola* giant axons. This sigmoidal time course of recovery from inactivation has been a consistent observation in twenty nodes. The recovery time course at three potentials is shown in Fig. 2. From such records a delay in recovery for each potential was estimated by plotting $-\ln(1-p)$ as a function of time, where $p(t) = I^t_{Na}/I^\infty_{Na}$ and I^t_{Na} and I^∞_{Na} are peak sodium currents in the test pulse at recovery intervals t and 200 msec respectively. If the recovery time course were a single exponential, where $p = 1-\exp(-t/\tau_h)$, the plot should yield a straight line passing through the origin. However, plots of observed $-\ln(1-p)$ *vs.* time (Fig. 3) show clear deviations from a straight line, with the recovery relaxing into a single exponential only at times longer than approximately 6 msec. A straight line was fitted to the late recovery

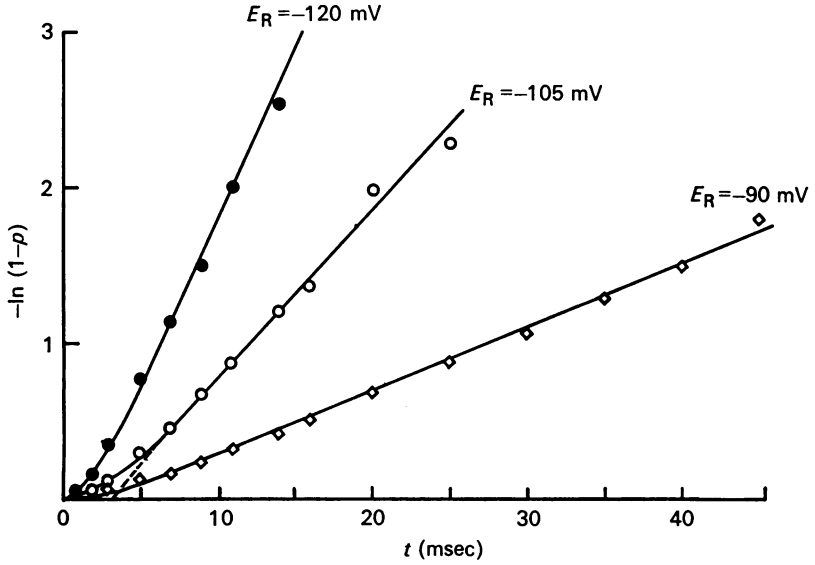

Fig. 3. Recovery from inactivation. Same data as in Fig. 2 but plotted semilogarithmically. Abscissa: as in Fig. 2. Ordinate: $\ln(1-p)$, where $p = I^{test}_{Na}/I^\infty_{Na}$, currents as defined in Fig. 2.

points and the slope was a measure of the final relaxation time constant τ_h at every potential. The intercept of this straight line with the time axis is taken as a measure of the 'delay' in recovery from inactivation. This delay has values on the order of 2–4 msec and depends on the recovery potential, being smaller for more hyperpolarizing potentials (Fig. 4). For potentials depolarizing with respect to rest, the steady-state inactivation

falls steeply to zero as a function of voltage, but, for a very narrow range of depolarizing potentials in which the currents are large enough for analysis, the delay was found to decrease with more depolarizing voltage. In two experiments, the delay of recovery from inactivation at a given recovery potential was found not to depend significantly on the prepulse potential so long as the prepulses inactivated the sodium current completely. The voltage dependence of the time constant τ_h of the later phase of recovery kinetics is shown in Fig. 5 (open circles).

Development of inactivation

During a maintained depolarization under voltage clamp, sodium current rises sharply and then decays slowly. In all my nodes, this decay phase is not a single exponential (Fig. 6). If analysed in terms of a linear summation of exponentials, the decay phase (Fig. 7*A*) is multi-exponential but it is not possible to tell from the decay whether two or more exponentials are needed to fit the time course. However, it seems natural to

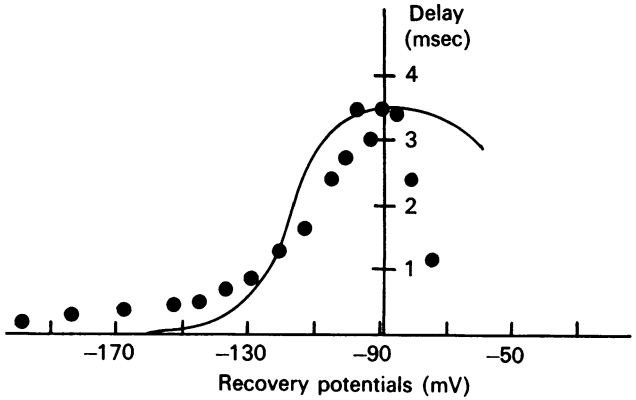

Fig. 4. Delay in recovery from inactivation (ordinate) *vs.* membrane potential (abscissa). The continuous line was calculated according to eqn. (15). In determining the delay, a straight line was fitted to the late recovery points plotted in Fig. 3, and the intercept on the time axis was taken to be the delay. The dotted line in Figs. 2 and 3 shows such an extrapolation for the delay at $E_R = -105$ mV.

start the analysis using two exponentials. Irrespective of the physical models proposed for inactivation, then, the time course of inactivation can be represented mathematically by the general equation

$$I_{Na}(\text{decay}) = A \exp(-k_1 t) + B \exp(-k_2 t) \quad (k_2 < k_1).$$

Qualitatively, then, sodium currents decay with a fast phase (characterized by the rate constant k_1) giving way to a slower phase (characterized by the rate constant k_2). These rate constants can be determined from plotting

the logarithm of sodium current against time (Fig. 7*B*). From the semilogarithmic plot in Fig. 7*B*, it can be seen that the data points do not fit a single straight line and two straight lines with different slopes can be fitted by eye to the data points corresponding to an initial fast phase (k_1) and a final slower phase (k_2). The value of k_2 obtained from semilogarithmic plots was found to be comparable to that obtained from a least squares fit of the above function to the sodium current decay by a computer. Experiments like that of Fig. 6*A* show that A and B of the above equation, which determine the relative contribution of the two phases,

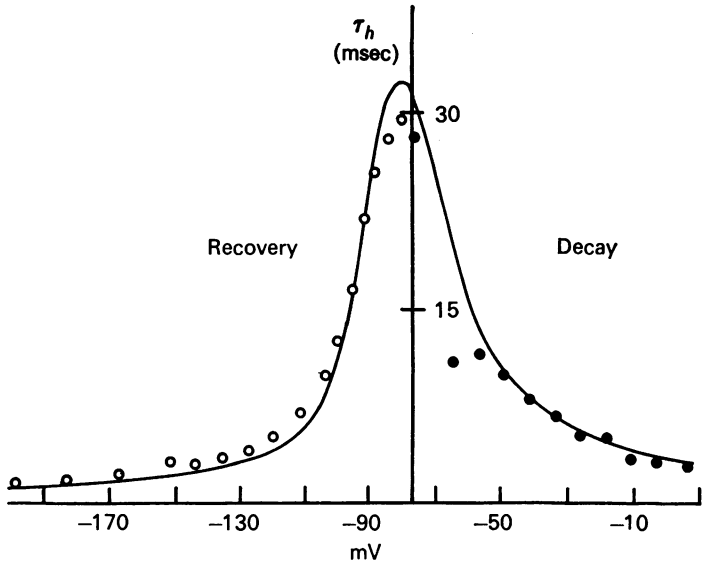

Fig. 5. Final time constants of inactivation (τ_h) *vs.* membrane potential. Points (open circles) to the left of the ordinate obtained from recovery experiments as in Fig. 3. Points (filled circles) to the right of the ordinate represent the final time constants determined from decays of sodium current under a maintained depolarization. Note that the peak of the τ_h curve is about 7 mV to the right of that of the delay curve (Fig. 4). The solid line was calculated according to eqn. (8).

are voltage dependent. The two time constants were clearly separated out around moderate depolarizing potentials, e.g. −26 mV. However, at extreme depolarizing potentials, the fast phase begins to dominate while the second phase disappears ($B \to 0$), and the decay of sodium current approaches a single exponential, e.g. at +14 mV.

Estimation of the second time constant (k_2) at extreme depolarizations is, thus, impossible. Even around moderately depolarized potentials where biphasic inactivation is most prominent, quantitative determination

of the second time constant is still unreliable up to a factor of 2 since the second component becomes evident only when inactivation of sodium current has proceeded to within 15–20 % completion.

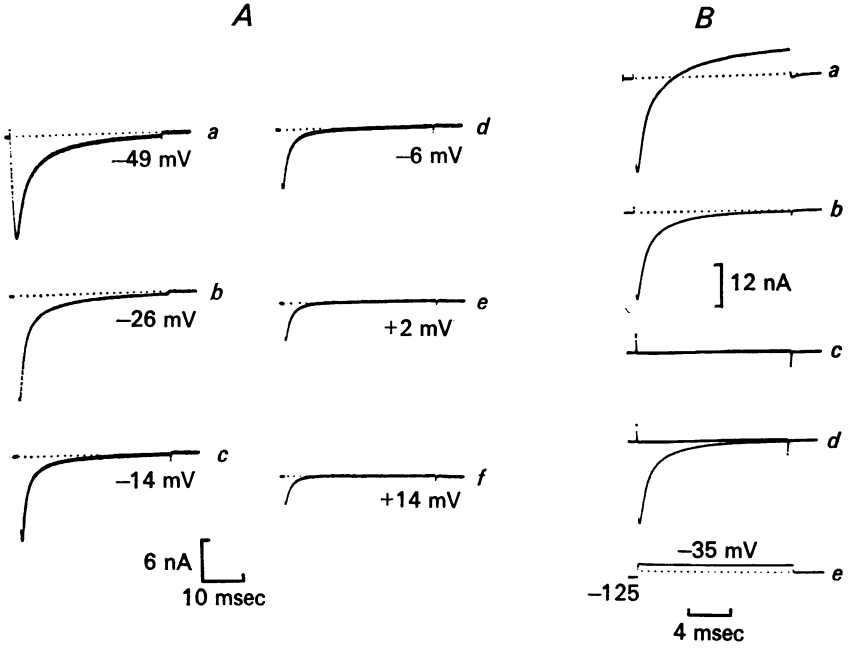

Fig. 6. Time course of the ionic currents through the nodal membrane after leak and capacitative subtraction. Part *A*, *a–f* show a family of sodium currents under different maintained depolarizations. Each depolarization was preceded by a 50 msec, −125 mV hyperpolarization to remove resting inactivation. Potassium currents were blocked by internal and external application of TEA-Cl (see Methods). Node 97. Resting potential, −87 mV. Temperature 4·5 °C. Part *B*, membrane depolarized to −35 mV. The voltage trace is shown at the bottom. *a*, normal Ringer without TEA, showing the initial inward sodium current and late outward potassium current. *b*, external application of 12 mM-TEA-Cl to Ringer. *c*, external application of 12 mM-TEA-Cl plus 500 nM tetrodotoxin (TTX) to Ringer. *d*, superimposed records from *b* and *c*. The ends of this node were cut in 120 mM-KCl. Node 100. Resting potential, −81 mV. Temperature 10 °C. Notice that inactivation of sodium current is not a single exponential, but, rather, biphasic (*Bb*, *Bd*, *Aa* to *Ac*). This biphasic nature of inactivation is most prominent from −49 to −14 mV (*Aa* to *Ac*). At high depolarizations (+14 mV, *Af*), the second slower phase disappears leaving only a single exponential inactivation of the sodium current.

Series resistance

Series resistance problems may affect the time course of the sodium transient and it must be questioned whether it is possible to account for the observed splitting of the decay into two time constants by the existence of a series resistance between the sodium channel and the bath electrode. This error is now considered in detail.

I have done computer simulations of a nerve model obeying the Hodgkin–Huxley kinetics but with a series resistance between the sodium channel and the bathing solution. Using the value of 100 kΩ for the series resistance from Dodge (1963) and solving the time course of the sodium transient with and without the series resistance, I found that series resistance cannot account for the observed non-exponential decay of the sodium transient. At a given potential within the positive limb of the current–voltage relation for the sodium current, increasing the series resistance decreases the peak of the sodium transient without much effect on the time course. In order to test experimentally the possibility of series resistance error, I lowered the external sodium concentration from 115 to 50–25 mM by equimolar substitution of NaCl by TMA-Cl and observed that this procedure did not eliminate the biphasic nature of inactivation development under a maintained depolarization. In fact, at the same potential, the ratio of the initial fast time constant to the final time constant remains fairly invariant with respect to the external sodium concentration used (Fig. 8).

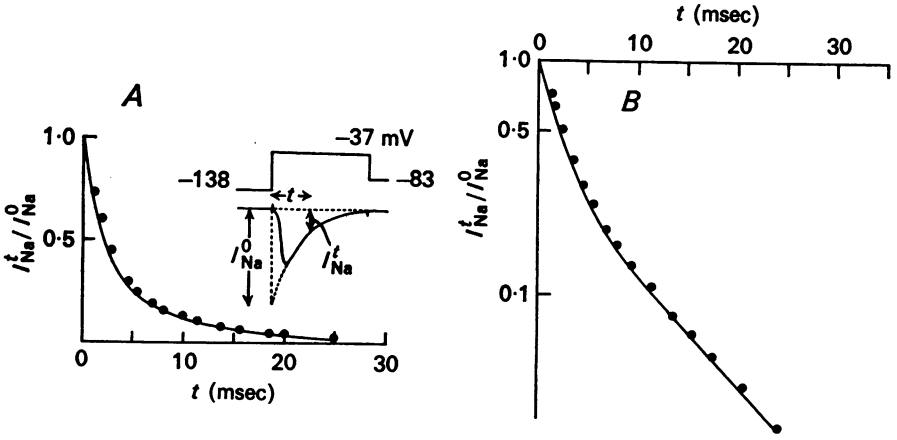

Fig. 7. *A*, development of inactivation at −37 mV. The decay portion of the sodium current trace was normalized with respect to I^0_{Na}, the value obtained by extrapolating the current trace back to the onset of the maintained depolarization. The depolarization was preceded by a 50 msec hyperpolarization to −138 mV to remove any resting inactivation. Continuous line was calculated by eqn. (16). *B*, development of inactivation at −37 mV plotted semilogarithmically. Ordinate: ln (I^t_{Na}/I^0_{Na}). Abscissa: time in msec after onset of depolarization. Node 58. Temperature 4·5 °C.

Leak current

Another possibility to account for the non-exponential time course of inactivation development is that the leak may be non-linear, whereas in my work I assumed a linear leakage correction. This was checked by using 500 nM-TTX to block all the sodium current and plotting the current–voltage relation for the leak. The current–voltage relation was linear over the potential range from the holding potential to −50 or −30 mV where non-exponential development of inactivation was most obvious. Finally, the time course of the leakage current under a maintained depolarization was checked for possible time-dependent rectification. Again, under TTX block, the time course of leakage current was observed in detail. At high depolarizing potential (to above 0 mV), the current was not a square step but increased towards

the end of the depolarization. This time-dependent rectification of the currents under TTX and TEA block did not occur at lower depolarizing potentials (− 80 to − 30 mV), however, and, therefore, would not affect the measurement of the second relaxation time constant in the decay of sodium current over these potential ranges (see traces *c* and *d* of Fig. 6*B*).

The time course of development of inactivation can also be determined by the double pulse method (see Methods) which is a completely inde-

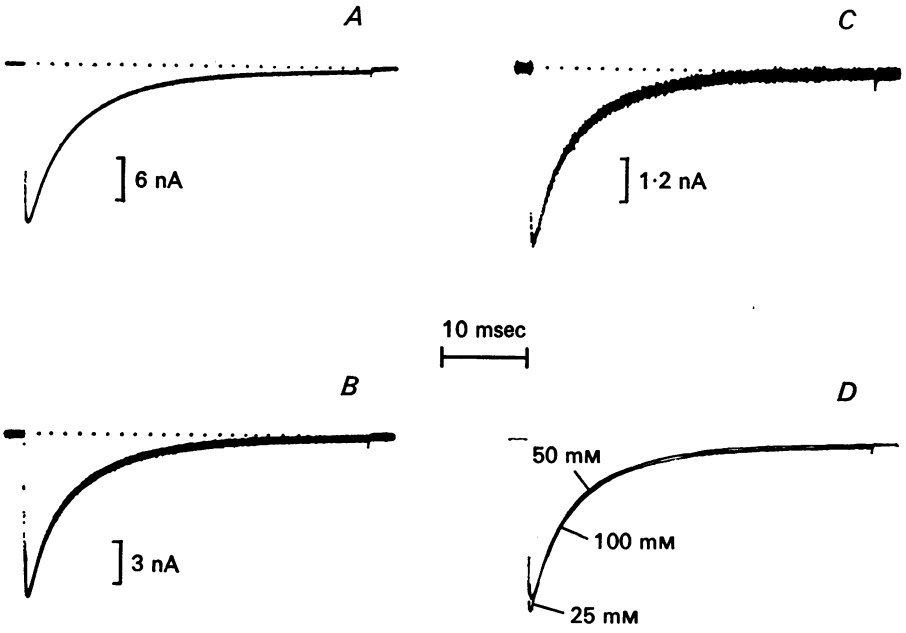

Fig. 8. Effect of changing external sodium ion concentrations on the time course of sodium current inactivation. *A–C* show inactivation of sodium current under a maintained depolarization to − 30 mV with different external sodium concentrations (see Methods). The external sodium concentration is: 115 mM in *A*, 50 mM in *B* and 25 mM in *C*. These current traces were photographed directly from the oscilloscope and were deliberately scaled to the same peak height so they can be superimposed on each other, as shown by the hand-traced records in *D*. Note that the biphasic time course of sodium inactivation is not affected by changing external sodium concentration.

pendent measurement from that of directly observing the decay of the sodium transient. According to the Hodgkin–Huxley formalism, the time constants of inactivation development determined by these two methods should agree. Recently, Goldman & Schauf (1973) found that, in *Myxicola* giant axon, measurement by these two methods results in different values for the time constants of inactivation development. In my experiments,

the time course of inactivation development measured by the double pulse method is similar to the time course of decay of the sodium current (Fig. 9). Fig. 9*B* shows normalized time courses of inactivation development measured by the two different methods. Although the time courses may differ slightly, their time constants would definitely not differ from each other by more than 20%. This comparison of the time constants was made over a voltage range from rest (−80 mV) to −35 mV,

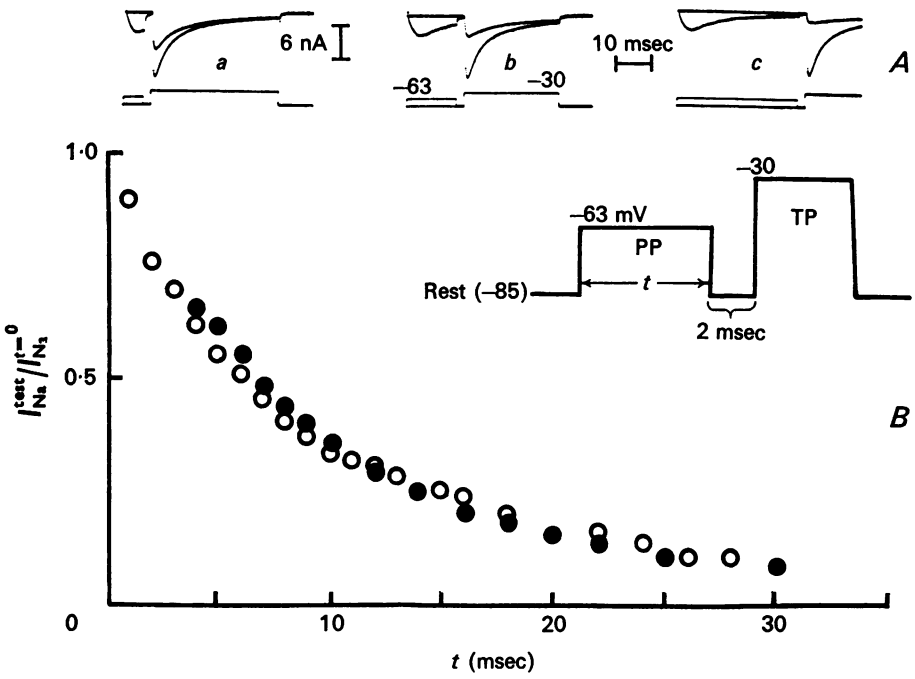

Fig. 9. Comparison of time courses of inactivation at −63 mV measured by two different methods on the same node. Part *A*, *a–c* show three records from the two-pulse method. In each record, the upper trace is current and lower trace is voltage. A test pulse (TP) was applied at *a*, 5 msec; *b*, 13 msec; *c*, 32 msec after the onset of a −63 mV prepulse (PP). Two different current traces were superimposed for each test pulse, one trace with the prepulse on and the other with the prepulse off. The test sodium current with the prepulse off (the larger current trace for each test pulse) was used as a control. With the prepulse on, the rate of decline of peak sodium current in the test pulse as a function of prepulse duration gives a measure of the time course of inactivation induced by the prepulse. Alternatively, this time course can also be observed directly from the decay of sodium current during the prepulse as in *c*. Part *B*, a quantitative analysis of the experiment in *A*. ○, development of inactivation at −63 mV measured by the two-pulse method. ●, normalized time course of decay of sodium current under the maintained depolarization at −63 mV. Node 60. Resting potential, −85 mV. Temperature, 4·5 °C.

and no significant discrepancies were found. The agreement of the two methods of measurement argues against artifacts of the measuring system as the cause of the biphasic time course.

It is possible that still longer time constants exist in the decay of the sodium transient and are undetected due to the closeness to the base line. However, over the time range under a maintained depolarization where

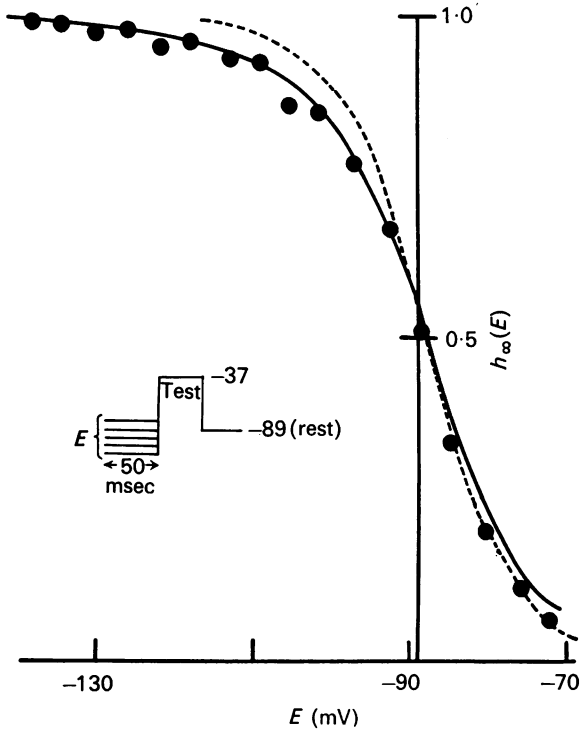

Fig. 10. Steady-state inactivation, h_∞, *vs.* membrane potential. Ordinate: $h_\infty(E) = I_{Na}^{test}(E)/I_{Na}^{max.}$, where $I_{Na}^{test}(E)$ is the peak sodium current in the test pulse after various prepulses of 50 msec duration. $I_{Na}^{max.}$ is the peak sodium current in the test pulse corresponding to a maximal hyperpolarizing prepulse. Abscissa: E, prepulse potential in mV. Dashed curve: $1/[1+\exp(AE+B)]$ with coefficients A and B extrapolated from data points to the right of −93 mV. Continuous curve: fit to the data using the equation $1/[1+\exp(A_1E+B_1)+\exp(A_2E+B_2)]$, with coefficients A_1, A_2, B_1, and B_2 calculated from eqn. (9) and rate constants from eqns. (10)–(13).

the current size is sufficiently large for semilogarithmic analysis, the two phases discussed seem prominent. The second relaxation time constant for development of inactivation has the potential dependence shown in Fig. 5 (filled circles).

Steady-state inactivation

The steady-state value of inactivation was measured by the traditional method of determining the peak sodium current in a test pulse applied after a 50 msec prepulse to various potentials (Hodgkin & Huxley, 1952*a*). As the prepulse was made more hyperpolarizing, inactivation was reduced and the evoked sodium current became larger until it finally saturated at extreme hyperpolarization. The saturating sodium current was then used to normalize the test sodium currents resulting from other prepulse potentials. A plot of the normalized peak currents against the prepulse potential gives the familiar function $h_\infty(E)$ (see Fig. 10) which I will interpret as

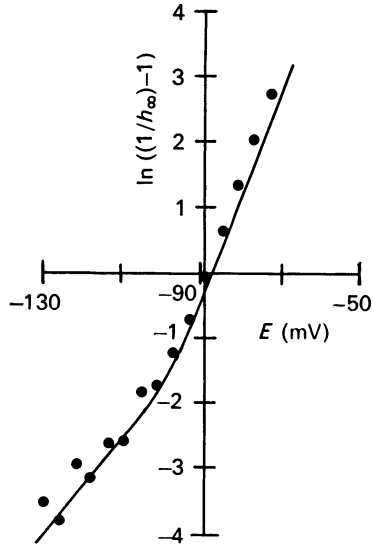

Fig. 11. Voltage dependence of steady-state inactivation. Same data as in Fig. 10 but plotted differently. Ordinate: $\ln [\{1/h_\infty(E)\}-1]$. Abscissa: prepulse potential. Using this plot, $1/[1+\exp(AE+B)]$ and

$$1/[1+\exp(A_1E+B_1)+\exp(A_2E+B_2)]$$

become $AE+B$ and $A_1E+B_1+\ln[1+\exp\{(A_2-A_1)E+(B_2-B_1)\}]$, respectively, with $A_{1,2}$ and $B_{1,2}$ calculated from eqn. (9). Note the nonlinearities exhibited by the data (●), and the continuous line.

a measure of the steady-state occupancy of the open state of the h system. In all the nodes studied, the $h_\infty(E)$ curves were not symmetrical. Asymmetries can be defined by plotting the quantity $\ln [\{1/h_\infty(E)\}-1]$ against voltage. For a symmetrical $h_\infty(E)$ with the form

$$h_\infty(E) = 1/[1+\exp(AE+B)],$$

this plot would yield a straight line. Such a plot is shown in Fig. 11. Since the plot is not a straight line, the observed $h_\infty(E)$ is not symmetrical. This finding is reproducible from node to node.

A three-state model for the inactivation system

It appears that my observations are not consistent with the interpretation of the Hodgkin–Huxley formalism that the inactivation h system has only two states. In the Hodgkin–Huxley scheme, the inactivation system can either be in one of two states, kinetically related by the scheme

$$\underset{0}{\text{open}} \quad \underset{\alpha_{01}}{\overset{\alpha_{10}}{\rightleftharpoons}} \quad \underset{1}{\text{closed}}$$

where the rate constants a_{01} and a_{10} depend on potential only. The time course of occupancy of the open state can be obtained by solving the equation

$$\frac{dP_0(t)}{dt} = -P_0(t)\, a_{01} + a_{10}[1 - P_0(t)],$$

where $P_0(t)$ denotes the fractional occupancy of the open state as a function of time. At any voltage, the solution of the above equation gives strictly exponential time courses of transition between the open and closed state, in contrast to my observations on development and recovery of inactivation. The delay in recovery from inactivation, in particular, suggests that there is an additional closed state of the inactivation system such that a transition between the two adjacent closed states delays the time course of recovery from inactivation. While other schemes may account equally well for the above kinetic observations, I have worked on a relatively simple physical model of the inactivation system suggested to me by Dr C. F. Stevens. This model assumes that the inactivation gate has three states, one open and two closed in a linear sequence.

$$\underset{0}{\text{open}} \quad \underset{\alpha_{01}}{\overset{\alpha_{10}}{\rightleftharpoons}} \quad \underset{1}{\text{closed}} \quad \underset{\alpha_{12}}{\overset{\alpha_{21}}{\rightleftharpoons}} \quad \underset{2}{\text{closed}}$$

The rate constants associated with transitions between adjacent states are voltage dependent and are assumed to be given by

$$a_{ij} = \exp(A_{ij}E + B_{ij}), \tag{1}$$

where A_{ij} and B_{ij} are constants (Magleby & Stevens, 1972).

Using eqn. (1) for the rate constants, the next step is to solve for the time course of and steady-state occupancy in the open state which are the measurable parameters in our experiments. If we let $P_1(t)$ denote the

probability of occupancy in state i at time t, then for each state we can write the following equations.

$$dP_0(t)/dt = a_{10}P_1(t) - a_{01}P_0(t), \tag{2}$$

$$dP_1(t)/dt = a_{01}P_0(t) - (a_{10}+a_{12})\,P_1(t) + a_{21}P_2(t), \tag{3}$$

$$dP_2(t)/dt = a_{12}P_1(t) - a_{21}P_2(t). \tag{4}$$

Imposing the constraint that $P_0(t)+P_1(t)+P_2(t) = 1$, then $P_1(t)$ and $P_2(t)$ can be eliminated from the above equations to give an explicit differential equation for $P_0(t)$, the fractional occupancy in the open state.

$$d^2P_0(t)/dt^2 + C_2\,dP_0(t)/dt + C_1P_0 + C_0 = 0, \tag{5}$$

where

$$C_2 = a_{10}+a_{01}+a_{12}+a_{21},$$

$$C_1 = a_{10}a_{21}+a_{21}a_{01}+a_{12}a_{01},$$

$$C_0 = -a_{21}a_{10}.$$

The general solution for $P_0(t)$ is

$$P_0(t) = P_0(\infty) + G_1 \exp(-k_1 t) + G_2 \exp(-k_2 t), \tag{6}$$

where

$$k_1 = [C_2 + \sqrt{(C_2^2 - 4C_1)}]/2, \tag{7}$$

$$k_2 = [C_2 - \sqrt{(C_2^2 - 4C_1)}]/2, \tag{8}$$

$$P_0(\infty) = 1/[1 + (a_{01}/a_{10}) + (a_{01}a_{12}/a_{10}a_{21})],$$

$$G_1 = [(a_{10}+a_{01}-k_2)\,P_0(0) + a_{10}P_2(0) - a_{10} + k_2P_0(\infty)]/(k_1-k_2),$$

$$G_2 = P_0(0) - P_0(\infty) - G_1.$$

k_1 and k_2 are the two rate constants in every kinetic response, $P_0(0)$ and $P_2(0)$ denote the initial conditions and $P_0(\infty)$ is the steady-state value for every response. Eqn. (6) says that the time course of fractional occupancy in the open state for a given potential is not a single exponential, but, since $k_1 > k_2$, will always relax with a final time constant $1/k_2$ for long times. Thus, k_2 can be measured as a function of voltage by determining the final relaxation time constants from the recovery and decay experiments. According to eqn. (8), k_2 is a function of all the a_{ij}s since C_2 and C_1 in that equation are functions of a_{ij}s. It can be shown, however, that, at extreme potentials, k_2 approaches one single a_{ij} and, therefore, empirical determination of $k_2(E)$ over a wide range of potentials will yield useful information on a_{ij}s. As will be seen shortly, this empirical determination of $k_2(E)$, coupled with the measured steady-state occupancy in the open state $h_\infty(E)$, gives enough constraints to determine all the rate constants a_{ij}s which should be necessary and sufficient to reproduce all the kinetic observations made in this paper.

The steady-state occupancy in the open-state 0 as a function of potential is given by the equation

$$h_\infty(E) = P_0(\infty) = 1/[1+(a_{01}/a_{10})+(a_{01}a_{12}/a_{10}a_{21})] \quad (9)$$

and $\ln[\{1/h_\infty(E)\}-1] = \ln(a_{01}/a_{10})+\ln[1+(a_{12}/a_{21})]$.

Thus, according to this model, $\ln[\{1/h_\infty(E)\}-1]$ has two asymptotes, $\ln(a_{01}/a_{10})$ at very negative potentials and $\ln(a_{01}/a_{10})+\ln(a_{12}/a_{21})$ at strong depolarizations (assuming that, for extreme hyperpolarization, $a_{21} \gg a_{12}$ and, for extreme depolarization, $a_{12} \gg a_{21}$). This is at once qualitatively in agreement with the observed plot of $\ln[\{1/h_\infty(E)\}-1]$, as shown in Fig. 11. The solid line in that figure was calculated according to eqn. (9) using the rate constants given in eqns. (10)–(13).

Determination of the rate constants a_{ij}

From the above consideration, the values of $\ln(a_{01}/a_{10})+\ln(a_{12}/a_{21})$ and $\ln(a_{01}/a_{10})$ were obtained from the two asymptotes of the plot of observed $\ln[\{1/h_\infty(E)\}-1]$ over opposite potential extremes. Other constraints on possible values of a_{ij}s can be obtained by plotting

$$\ln[1/(\text{final time constant }(E))] = \ln[k_2(E)]$$

vs. potentials and measuring the two asymptotes over opposite extreme potentials. It can be shown that over the hyperpolarizing range the asymptote approaches either a_{10} or a_{21}. In the analysis, the choice a_{10} was used since it resulted in better fit to the data. Over extreme depolarizations, the asymptote should yield a_{12}, but a further clarification of this point is needed. The time course of inactivation at moderate to extreme depolarizations can be approximated to an excellent degree by eqn. (16). Using the simple assumptions that at high depolarizations $a_{01} \gg a_{10}$ and $a_{12} \gg a_{21}$, and using eqns. (7) and (8) for k_1 and k_2 respectively, it can be shown that as E becomes large (extreme depolarization), either $k_1 \to a_{01}$ and $k_2 \to a_{12}$ *or* $k_1 \to a_{12}$ and $k_2 \to a_{01}$. Examination of the family of sodium currents in Fig. 6*A* reveals that the time course of inactivation, which is clearly biphasic at moderate depolarizations, becomes a single exponential at high depolarizations as the second phase begins to disappear, implying that the coefficient $(a_{01}-k_1)/(k_2-k_1)$ in eqn. (16) approaches zero at high potentials. Thus, the choice $k_1 \to a_{01}$ and $k_2 \to a_{12}$ at large depolarizations seems correct and the asymptote of the plot $\ln(k_2)$ *vs.* potential at extreme depolarizations should yield a_{12}. In practice, however, it is impossible to resolve k_2 at extreme depolarizations and extrapolation for a_{12} on the plot $\ln(k_2(E))$ can only be done within the narrow range of moderate depolarizations over which the asymptote is only just beginning to form and there still

remains enough resolution of the two time constants in the decay of sodium currents. Thus, from the plots of the observed ln $[\{1/h_\infty(E)\}-1]$ and ln $[k_2(E)]$ *vs.* voltage, first estimates for the four rate constants were quickly determined. The accuracies of these estimates were checked by calculating the $h_\infty(E)$ and $k_2(E)$ corresponding to these rate constants using eqns. (8) and (9). The $h_\infty(E)$ and $k_2(E)$ values calculated were compared with the observed values and discrepancies were reduced by manually adjusting the first chosen set of rate constants. Usually the final set did not differ much from the initial set chosen. The final set of rate constants for node 38 (at a temperature of 4·5 °C and in msec^{-1}) is given by

$$a_{12} = \exp(0{\cdot}013E - 1{\cdot}4), \tag{10}$$

$$a_{01} = \exp(0{\cdot}05E + 1{\cdot}0), \tag{11}$$

$$a_{21} = \exp(-0{\cdot}102E - 11{\cdot}9), \tag{12}$$

$$a_{10} = \exp(-0{\cdot}015E - 2{\cdot}96), \tag{13}$$

where E is the absolute membrane potential in millivolts. This set of rate constants should completely define all the kinetic responses under the various experimental conditions in this paper if the model is a reasonably accurate approximate description of the actual physical mechanism.

Fitting of the model to the observations

The first test of this model is to see if the chosen set of rate constants (eqns. (10)–(13)) reproduces appropriate values for the observed delays in recovery from inactivation. The experimental conditions for recovery from inactivation can be imitated by using the initial conditions $P_0(0) = 0$, $P_1(0) = 0$ and $P_2(0) = 1$ for eqn. (6) and the time course of recovery becomes

$$P_0(t)/P_0(\infty) = 1 + [k_2/(k_1 - k_2)] \exp(-k_1 t) + [k_1/(k_2 - k_1)] \exp(-k_2 t). \tag{14}$$

The delay (as defined in the Methods) can be deduced from eqn. (14) to have the following potential dependence:

$$\text{delay} = (1/k_2) \ln [k_1/(k_1 - k_2)]. \tag{15}$$

In Fig. 4, the continuous line shows the calculated delay (according to eqn. (15)) as a function of recovery potential, and Figs. 2 and 3 show various calculated recovery time courses (according to eqn. (14)) as a function of different recovery potentials.

The experimental conditions for development of inactivation under various maintained depolarizations preceded by a large hyperpolarizing prepulse to remove resting inactivation can be imitated by the initial conditions $P_0(0) = 1$, $P_1(0) = P_2(0) = 0$. Eqn. (6), with these initial conditions, becomes

$$P_0(t) = P_0(\infty) + [(a_{01} + k_2 P_0(\infty) - k_2)/(k_1 - k_2)] \exp(-k_1 t) + (a_{01} - k_1 + k_1 P_0(\infty))/(k_2 - k_1)] \exp(-k_2 t).$$

For moderate to high depolarizations which completely inactivate the sodium current ($P_0(\infty)$ approaches zero), the time course of inactivation can be approximated by

$$P_0(t) = [(a_{01}-k_2)/(k_1-k_2)] \exp(-k_1 t) + [(a_{01}-k_1)/(k_2-k_1)] \exp(-k_2 t). \quad (16)$$

Eqn. (16) was used to calculate the time course of inactivation at -37 mV, as shown by the solid line in Fig. 7. Figs. 2–5 and Figs. 7, 10 and 11 show a summary of all the calculated kinetic responses superimposed on the actual observations. It should be emphasized that only the values of rate constants given in eqns. (10)–(13) were used to make predictions shown in all Figures; no adjustable parameters were used to alter the fit for individual Figures.

DISCUSSION

The primary results of this paper show that neither inactivation nor recovery from it in the sodium channel can be described in terms of a single first order differential equation. The critical evidence is that the time course of transitions of the inactivation system between its open and closed states is not a simple exponential, as shown in Figs. 1*B*, 2, 6 and 7. The delay in recovery from inactivation was first reported by Schauf (1974). The delays reported in this paper at a temperature of 4·5 °C are in the order of 2–4 msec, in good agreement with Schauf's (1974) results on *Myxicola*. One interesting feature of the voltage dependence of the delay is observed. The delay (E) curve (Fig. 4) has a bell shape with its peak displaced slightly to the hyperpolarizing direction relative to the peak of the $\tau_h(E)$ curve along the voltage axis. From Dodge (1963) the bell-shaped $\tau_m(E)$ curve has its peak displaced to the depolarizing direction relative to the $\tau_h(E)$ curve. This implies that, over a certain potential range, the delay in recovery from inactivation decreases with potential while the τ_m increases. If the delay in recovery is a result of coupling between the activation and inactivation processes, then the above observation means that the nature of coupling must be more complicated than that implied by the correlation between $\tau_m(E)$ and the delay in development of inactivation reported by some authors (Goldman & Schauf, 1972; Schauf & Davis, 1975). Calculation from the model shows that the peak of the delay-in-recovery (E) curve should always be slightly hyperpolarizing relative to the peak of the $\tau_h(E)$ curve, in agreement with the observations.

The observation that the decay of the sodium current under a maintained depolarization exhibits at least two time constants is direct evidence for second order properties in the inactivation system. The fact that this

multi-exponential time course remains invariant with respect to external sodium concentration and the methods used to measure them tends to rule out the possibility of an experimental artifact.

One of the major arguments against the Hodgkin–Huxley formalism of two separate processes, activation and inactivation, governing the opening and closing of the sodium channel is that the time constant of development of inactivation measured from decay of sodium transients differs from that measured by the conditioning pulse method (Goldman &

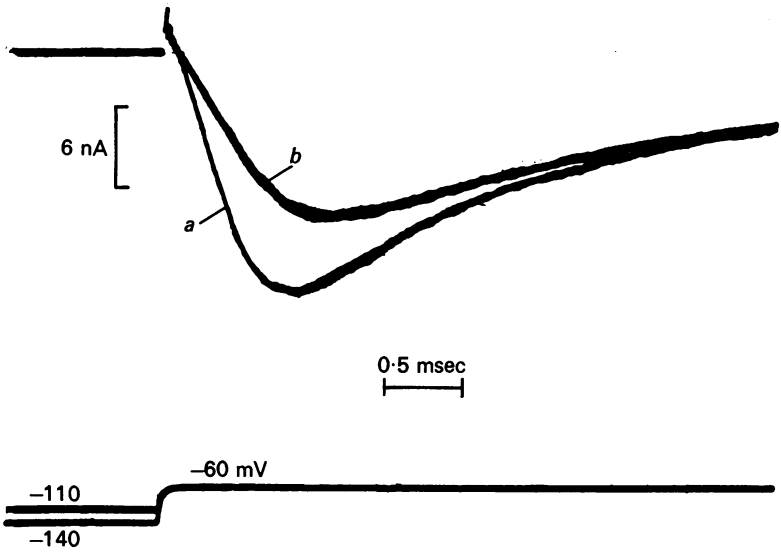

Fig. 12. Slowing down of turn-on of sodium current in a −60 mV test pulse by strong hyperpolarizing prepulse. Upper traces, current. Lower traces, voltage. The test pulse used fell within the negative slope region of the *I–E* plot for sodium current. Trace *a* shows sodium current in the test pulse with a 50 msec, −110 mV hyperpolarizing prepulse. Only the last 1 msec of the hyperpolarizing prepulse is shown. In *b*, the hyperpolarizing prepulse was −140 mV. Instead of evoking a bigger sodium current, the stronger hyperpolarizing prepulse actually results in smaller peak current in the test pulse. This may be the result of a slowing down of the turn-on of the sodium current in the test pulse by the −140 mV hyperpolarizing prepulse. Node 100. Resting potential, −81 mV. Temperature 10 °C.

Schauf, 1973; Goldman, 1975). It appears that in nodes these differences in time constants are lacking. It is still not clear why these differences in time constants are seen in *Myxicola* and not in nodes (Schauf, Pencek & Davis, 1976).

Another argument for coupling of activation to inactivation is the reported shift of the $h_\infty(E)$ curve along the voltage axis as a function of

the test pulse used (Hoyt & Adelman, 1970; Goldman & Schauf, 1972). I have tried to repeat this observation in nodes. However, this type of experiment is hindered by the following phenomenon. If a test pulse is used which falls within the negative slope region of the *I–E* plot for sodium currents, the turn-on of the sodium transient in the test pulse is slowed down considerably by strong hyperpolarizing prepulses (Fig. 12). This slowing down of the turn-on affects the peak height of the sodium current in the test pulse and extreme hyperpolarization could actually decrease rather than saturate the sodium current in a test pulse applied after the hyperpolarization (Dubois & Bergman, 1971). This phenomenon means that, if the $h_\infty(E)$ is measured using a test pulse falling within the negative slope region of the *I–E* plot, the saturating sodium current in the test pulse cannot be defined and the $h_\infty(E)$ curve cannot be normalized. Armstrong & Bezanilla (1974) also reported a delay in the turn-on of a sodium current after a strong hyperpolarization.

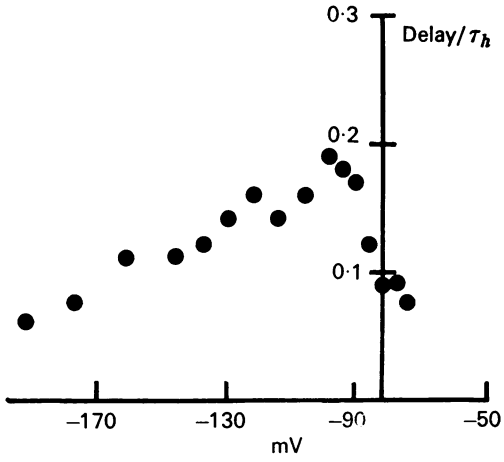

Fig. 13. (delay/τ_h) *vs.* absolute membrane potentials. ●, data averaged from four nodes. Ordinate: the ratio of the delay in recovery from complete inactivation to the final time constant of recovery. Abscissa: membrane potential in millivolts.

A family of the recovery curves at different potentials as shown in Fig. 2 greatly resembles the potassium currents with their sigmoidal time course and the possibility is raised of describing the inactivation system with kinetics of the type $[1-\exp(-t/\tau_h)]^n$, similar to the potassium system. For this type of kinetics, it can be shown that the ratio (delay/final relaxation time constant) for different recovery potentials should be a constant as a function of voltage, and equal to ln n. Fig. 13 shows the observed (delay/final relaxation time constant) as a function of the

recovery potentials. The ratio is not invariant with respect to potentials and, therefore, renders the potassium-type kinetics untenable. It is also interesting to note that in observations on nodes of Ranvier by Drs C. F. Stevens and T. Begenisich, the delay/final time constant for the potassium current is also not a constant function of potential (C. F. Stevens, personal communication).

Schauf (1976) recently reported that the time constants of reactivation and development of inactivation at the same potential are not the same. I have done one experiment in which the normalized time course of inactivation development and recovery from inactivation at the same potential were compared. In node, there is a narrow range of potentials over which the recovery after a large depolarization can be compared to the time course of development of inactivation after a strong hyperpolarization. The two time courses were not the same, with the recovery being a simple exponential, apart from a small initial delay while the development time course showed a slight biphasic behaviour. Calculation from the three-state model also showed these characteristics, but the calculated biphasic time course of development was less prominent than that observed over these potential ranges. The final relaxation time constants, for both development and recovery, however, were the same at the same potential, as observed.

The model does very well at predicting the time course of removal of inactivation, the time course of development of inactivation, and the steady-state voltage dependence of inactivation. The model is also qualitatively correct in predicting that at high depolarization sodium currents should decay with a single exponential (see the current trace at +14 mV in Fig. 6*A*) as according to eqn. (16) the amplitude coefficient of the slow phase, $(a_{01}-k_1)/(k_2-k_1)$, approaches zero. However, quantitatively, this coefficient approaches zero as a function of potential more steeply than is observed. In addition, the predicted time course of decay of the first phase becomes too fast – for example, a factor of 3 too fast at −5 mV. Both of these disagreements arise because the rate constant a_{01} depends too steeply on potential at high depolarizations. This suggests that the functional form used for the a_{1j}s (eqn. (1)) is oversimplified and other forms which saturate at high potentials might be preferable. Alternatively, adding more states to the model can help to make the fit better.

In summary, the kinetic observations reported in this paper show that the inactivation system has second order properties. While the present model does not give perfect fit, the approach gains merit from its simple mathematics and physical assumptions. The three-state inactivation model must be the simplest next alternative to the two-state inactivation model of Hodgkin and Huxley which definitely cannot account for the

observations. And, one of the tacit assumptions throughout the analysis is still the idea of two separate processes governing the sodium channel as first proposed by Hodgkin & Huxley (1952*a*).

I would like to thank Dr C. F. Stevens for initiating me in this project and deriving some of the equations. I am most grateful to Dr Bertil Hille for letting me work in his laboratory and giving me the most generous financial support, and to him, W. Almers, and C. F. Stevens for invaluable discussions throughout the various stages of this investigation. I also thank Dr Wolfgang Schwarz for help in using the computer for the least-squares fit on p. 580. Supported by grants NS08174 and FR00374 from the National Institutes of Health.

REFERENCES

ARMSTRONG, C. M. (1970). Comparison of gK inactivation caused by quaternary ammonium ion with gNa inactivation. *Biophys. J.* **10**, 185a.

ARMSTRONG, C. M. & HILLE, B. (1972). The inner quaternary ammonium ion receptor in potassium channels of the node of Ranvier. *J. gen. Physiol.* **59**, 388–400.

ARMSTRONG, C. M. & BEZANILLA, F. (1974). Charge movement associated with the opening and closing of the activation gates of the sodium channels. *J. gen. Physiol.* **63**, 533–552.

CHANDLER, W. K. & MEVES, H. (1970). Evidence for two types of sodium conductance in axons perfused with sodium fluoride solution. *J. Physiol.* **211**, 653–678.

CHIU, S. Y. (1976). Observation on sodium channel inactivation in frog nerve. *Biophys. J.* **16**, 25a.

DODGE, F. A. (1963). A study of ionic permeability changes underlying excitation in myelinated nerve fibres of the frog. Thesis, The Rockefeller University, University Microfilms, Inc., Ann Arbor (no. 64–7333).

DODGE, F. A. & FRANKENHAEUSER, B. (1958). Membrane currents in isolated frog nerve fibre under voltage clamp conditions. *J. Physiol.* **143**, 76–90.

DUBOIS, J. M. & BERGMAN, C. (1971). Sodium conductance of the nodal membrane: competitive inhibition between calcium and sodium. *C. r. hebd. Séanc. Acad. Sci., Paris* **272**, 2924–2927.

GOLDMAN, L. (1975). Quantitative description of the sodium conductance of the giant axon of *Myxicola* in terms of a generalized second-order variable. *Biophys. J.* **15**, 119–136.

GOLDMAN, L. & SCHAUF, C. L. (1972). Inactivation of the sodium current in *Myxicola* giant axons. Evidence for coupling to the activation process. *J. gen. Physiol.* **59**, 659–675.

GOLDMAN, L. & SCHAUF, C. L. (1973). Quantitative description of sodium and potassium currents and computed action potentials in *Myxicola* giant axons. *J. gen. Physiol.* **61**, 361–384.

HILLE, B. (1970). Ionic channels in nerve membrane. *Prog. Biophys. molec. Biol.* **21**, 1–32.

HILLE, B. (1971). The permeability of the sodium channel to organic cations in myelinated nerve. *J. gen. Physiol.* **58**, 599–619.

HILLE, B. (1976). Gating in sodium channels of nerve. *A. Rev. Physiol.* **38**, 139–152.

HODGKIN, A. L. & HUXLEY, A. F. (1952*a*). The dual effect of membrane potential on sodium conductance in the giant axon of *Loligo*. *J. Physiol.* **116**, 497–506.

HODGKIN, A. L. & HUXLEY, A. F. (1952*b*). A quantitative description of membrane current and its application to conduction and excitation in nerve. *J. Physiol.* **117**, 500–544.

HOYT, R. C. & ADELMAN, W. L. (1970). Sodium inactivation: experimental test of two models. *Biophys. J.* **10**, 610–617.

KOPPENHÖFER, E. & VOGEL, W. (1969). Effects of tetrodotoxin and tetraethylammonium chloride on the inside of the nodal membrane of *Xenopus laevis*. *Pflügers Arch. ges. Physiol.* **313**, 361–380.

MAGLEBY, K. L. & STEVENS, C. F. (1972). A quantitative description of end-plate currents. *J. Physiol.* **223**, 173–197.

PEGANOV, E. M. (1973). Kinetics of the process of inactivation of sodium channels in the node of Ranvier of frogs. *Bull. biol. Méd. exp. U.R.S.S.* **11**, 5–9.

SCHAUF, C. L. (1974). Sodium currents in *Myxicola* axons: non-exponential recovery from the inactive state. *Biophys. J.* **14**, 151–154.

SCHAUF, C. L. (1976). Comparison of two-pulse sodium inactivation with reactivation in *Myxicola* giant axons. *Biophys. J.* **16**, 245–248.

SCHAUF, C. L. & DAVIS, F. A. (1975). Further studies of activation–inactivation coupling in *Myxicola* axons: insensitivity to changes in calcium concentration. *Biophys. J.* **15**, 1111–1116.

SCHAUF, C. L., PENCEK, T. L. & DAVIS, F. A. (1976). Activation–inactivation coupling in *Myxicola* giant axons injected with tetraethyl-ammonium. *Biophys. J.* **16**, 985–989.